



Published in final edited form as:

Optom Vis Sci. 2014 July ; 91(7): 730–739. doi:10.1097/OPX.0000000000000304.

Guinea Pig Ciliary Muscle Development

Andrew D. Pucker, OD, MS, FAAO, Ashley R. Carpenter, BS, Kirk M. McHugh, PhD, and Donald O. Mutti, OD, PhD, FAAO

The Ohio State University College of Optometry (ADP, DOM), Biomedical Sciences Graduate Program (ARC, KMMc), and Nationwide Children's Hospital, Center for Molecular and Human Genetics, Columbus, Ohio (ARC, KMMc)

Abstract

Purpose—The purpose of this study was to develop a method for quantifying guinea pig ciliary muscle volume (CMV) and to determine its relationship to age and ocular biometric measurements.

Methods—Six albino guinea pigs eyes were collected at each of five ages (n=30 eyes). Retinoscopy and photography were used to document refractive error, eye size, and eye shape. Serial sections through the excised eyes were made and then labeled with an α -smooth muscle actin antibody. The CM was then visualized with an Olympus BX51 microscope, reconstructed with Stereo Investigator (MBF Bioscience) and analyzed using NeuroLucida Explorer (MBF Bioscience). Full (using all sections) and partial (using a subset of sections) reconstruction methods were used to determine CMV.

Results—There was no significant difference between the full and partial volume determination methods ($P = 0.86$). The mean CMV of the 1, 10, 20, 30, and 90-day old eyes was $0.40 \pm 0.16 \text{ mm}^3$, $0.48 \pm 0.13 \text{ mm}^3$, $0.67 \pm 0.15 \text{ mm}^3$, $0.86 \pm 0.35 \text{ mm}^3$, and $1.09 \pm 0.63 \text{ mm}^3$, respectively. CMV was significantly correlated with log age ($P = 0.001$), ocular length ($P = 0.003$), limbal circumference ($P = 0.01$), and equatorial diameter ($P = 0.003$). It was not correlated with refractive error ($P = 0.73$) or eye shape ($P = 0.60$). Multivariate regression determined that biometric variables were not significantly associated with CMV after adjustment for age.

Conclusions—Three-dimensional reconstruction was an effective means of determining CMV. These data provide evidence that CM growth occurs with age in tandem with eye size in normal albino guinea pigs. Additional work is needed to determine the relationship between CMV and abnormal ocular growth.

Keywords

myopia; refractive error; ciliary muscle; guinea pig; three-dimensional tissue reconstruction; ciliary muscle size; eye size; eye shape

Corresponding author: Donald O. Mutti, The Ohio State University, 338 West 10th Ave, Columbus, OH 43210, DMutti@optometry.osu.edu.

None of the authors has any personal financial relationships to disclose.

Over the years refractive error researchers have expended a great deal of effort and resources towards determining the full mechanism of emmetropization, eye growth that reduces neonatal hyperopia. In spite of this, the myopia research community is still unable to fully explain the mechanisms responsible for normal (emmetropic) and abnormal (e.g., myopic) eye growth. Nevertheless, some promising breakthroughs have come from work with animal models. For example, animal experiments have demonstrated predictable changes in eye growth from imposed optical defocus, with myopic defocus slowing eye growth and hyperopic defocus accelerating eye growth.¹⁻⁴ In spite of this evidence, treatments based upon reducing foveal defocus have resulted in little clinical benefit.⁵⁻⁷ In human clinical studies, the amount of defocus is not related to the risk of onset or the rate of progression of myopia,⁸ and correction of foveal defocus has not slowed myopic progression by a meaningful amount.^{6, 7} Therefore, additional factors must be involved in myopia development.

Recently, researchers have turned their attention to correcting peripheral hyperopic defocus.⁹ Specifically, investigators have found that reducing the peripheral hyperopic defocus found in the pre-myopic and post-onset eye,¹⁰ has decreased myopic progression by up to approximately 50% over a two year treatment period.^{11, 12} The source of relative peripheral hyperopia appears to be an alteration of eye shape from relatively oblate (wider than long) as seen in hyperopia and emmetropia to relatively prolate (longer than wide) as seen in myopia.¹³ While these results have produced insight into the underlying mechanism of myopia, they also raise the question of the source of this abnormal eye shape.

Recent data have suggested that one possible source is an abnormal ciliary muscle. Oliveira and coworkers and Bailey and coworkers have found that myopic adults and children have thicker ciliary bodies and muscles, respectively, particularly posteriorly, than hyperopic subjects.^{14, 15} These differences may have functional and structural consequences. Specifically, myopic children have an altered accommodative function consisting of an increased accommodative lag^{8, 16} and higher accommodative convergence to accommodation ratio (AC/A) compared to emmetropes.^{16, 17} The crystalline lens stops its normal thinning, flattening, and loss of power in myopic children at the time of myopia onset while these changes continue in subjects who remain emmetropic.^{18, 19} Losses in crystalline lens power counterbalance axial elongation to maintain emmetropia in childhood.^{18, 19} Together, these findings suggest that the enlarged ciliary muscle may impair the accommodative response to increase lag, create a pseudo-cycloplegia that increases the AC/A ratio, isolate the crystalline lens from the elongating eye, and mechanically restrict equatorial eye expansion to distort ocular shape and create peripheral hyperopic defocus. Any one or more of these factors could accelerate axial elongation and lead to myopia.^{14, 19}

All of the studies above relating the ciliary muscle to the development of myopia have been in humans. None of them have been able to provide a direct link between an altered ciliary muscle and myopic growth, and none of them have been able to elucidate an underlying biochemical or biomechanical process leading to this alteration in ciliary muscle structure and function. Therefore, development of a ciliary muscle measurement method in an animal model of myopia would be of value.

Over the years, myopia development has been studied in the chicken, tree shrew, monkey, rat, mouse, fish, rabbit, cat, guinea pig, and pig.^{20–23} While all of these animals have produced a better understanding of refractive error development, they also have their limitations. For example, primates are costly and reproduce slowly. Pigs have a minimal amount of ciliary muscle, a guinea pig's overlapping binocular vision field is limited compared to a human's (20° to 63° vs. 140° to 160°), and tree shrews are difficult to raise.^{20–22, 24, 25} Additionally, the chicken ciliary muscle is mostly skeletal muscle as opposed to smooth muscle as in mammalian eyes, and the anatomy and the mechanism of its accommodative system are different from that of a mammal.^{26, 27}

Of the animal models listed above, the guinea pig (*Cavia porcellus*) possesses several qualities that make it a reasonable choice for studying the ciliary muscle's involvement in myopia development. For example, the guinea pig myopia model is well characterized, a meaningful amount of myopia can be induced in a relatively short period of time, and myopia can be induced in a consistent and predictable manner.^{4, 28} Also, the guinea pig is known to be able to accommodate (Kisilak ML, et al. *IOVS* 2011: ARVO E-Abstract 845), yet its mechanism of accommodation may be different than that of primates because a guinea pig's accommodative system may be better suited for viewing near objects than a primate's system.^{29, 30} Furthermore, the guinea pig has more ciliary muscle tissue than other rodents (e.g., rat),³¹ and it develops and reproduces relatively quickly. The guinea pig's genome has been sequenced (6.76X coverage), which also makes it amenable to molecular biology experiments. Finally, laboratories have even taken steps to develop the guinea pig as a model for studying myopia control with bifocal contact lenses and orthokeratology lenses (Bowrey H, et al. *IOVS* 2013: ARVO E-Abstract 5176; Liu Y, et al. *IOVS* 2013: ARVO E-Abstract 5471).

To date, there is very little known about how a guinea pig's ciliary muscle develops and how this information is related to biometric measurements like refractive error. Therefore, the primary purpose of this study was to develop a means to quantifying the amount of ciliary muscle present in a guinea pig's eye, and to determine how a guinea pig's ciliary muscle size changes during the first 90 days of life. Preliminary results on how ciliary muscle growth is related to refractive error, eye size, and eye shape without experimental manipulation of visual experience are also presented. Ultimately, it is hoped that this information will contribute toward establishing the guinea pig as a suitable model for studying the role of the ciliary muscle in myopia.

METHODS

Subjects

Albino guinea pigs (*Cavia porcellus*) were bred from progenitors obtained from the Charles River Laboratory. They were raised in a 12-hour light/12-hour dark cycle environment. Eyes were collected at about 1, 10, 20, 30, and 90 days of age from twenty-one guinea pigs following carbon dioxide asphyxiation. The first six eyes collected at each time-point yielding high quality data were used in the analysis. Eyes that were unsuccessfully embedded and eyes that were damaged by microtome malfunctions were not used in the analysis. The Institutional Animal Care and Use Committee at The Ohio State University

approved this research, and it was in compliance with the Association for Research in Vision and Ophthalmology's Statement for the Use of Animals in Ophthalmic and Vision Research.

Refractive Error

Two-licensed optometrists measured refractive error with streak retinoscopy (ADP & DOM) 30 minutes after instilling two drops of 0.5% cyclopentolate (four total) five minutes apart in each eye. No fluctuations were seen in pupil size, accommodation, or refractive error during retinoscopy. Spherical equivalent refractive error was calculated from each investigator's measurements, and the mean of these two values was used in all subsequent analyses.

Ocular Size and Shape

Ocular length, equatorial diameter, and ocular shape (eye length/equatorial diameter) measurements were all derived from photographs of enucleated eyes (Figure 1). In brief, after enucleation, all loose tissue was removed and eyes were placed on a black background. Coronal view (front view) photos and transverse view (top view) photos of each eye were taken with a high-resolution black and white camera (SONY XC77). Each image had a resolution 27.9 pixels/mm. All images were then imported into ImageJ software. ImageJ was used to manually create best-fit circles in order to determine the ocular lengths, equatorial diameters, and limbal circumferences of the eyes (Figure 1). Circles were used instead of lines to measure axial length in order to make for easier identification of the distance between the anterior and posterior poles. Circles were also fit separately to the horizontal and vertical aspects of the coronal view and the limbus to determine if there was any asymmetry. Measurement reliability was determined by fitting each circle on 30 images on two different occasions.

Tissue Processing and Staining

Three-dimensional ciliary muscle reconstruction was performed by first fixing enucleated eyes with formalin for two days.³² The eyes were subsequently transferred to 70% ethanol until they underwent final processing with a Leica TP 1050 Tissue Processor (Leica Microsystems), which consisted of cycling the eyes through graded concentrations of alcohol and then xylenes followed by infusing them with paraffin wax. Eyes were then imbedded in blocks of paraffin wax and serial anterior to posterior plane sections through the entire eye were taken at 10 μ m increments. Sections were placed in a hot water bath and collected with Surgipath microscope slides (Leica-Microsystems, 3800200). The slides were then allowed to dry at room temperature overnight, and they were subsequently stored at room temperature until staining was performed.

Prior to staining, all slides were deparaffinized by first melting the paraffin wax with a 54°C slide warmer for at least five minutes. The wax was then removed, and the tissue was rehydrated by washing the slides with xylenes, 70% ethanol, and deionized water; each wash step was performed for five minutes. Antigen retrieval was then performed by transferring the slides to room temperature sodium citrate buffer (pH 6.0) and pressure-cooking them for 25 minutes. Slides were then slowly cooled and washed with deionized water followed by phosphate buffered saline (pH 7.2) (PBS) for five minutes each. Slides were then transferred

to hydrogen peroxide for 30 minutes; again they were washed in deionized water and PBS for five minute each.

Proteins were then blocked via a Biotin Blocking Kit (BBK120) and a Mouse-to-Mouse Blocking Kit (ScyTek Laboratories, MTM125) following the manufacturer's guidelines. The ciliary muscle was labeled with a primary α -smooth muscle actin antibody (Dako, M0851) at a 1:200 dilution for at least one-hour. Non-bound antibody was then washed off with a five-minute PBS wash. The antibody was then detected by first incubating the tissue with UltraTek Anti-Polyvalent (ScyTek Laboratories, ABN125) for 20 minutes and then with UltraTek horseradish peroxidase (HRP) (ScyTek Laboratories, ABL125) for 20 minutes; each of these solutions was also washed off with PBS for five minutes. The tissue was then subsequently incubated with 3-amino-9-ethylcarbazole (AEC) solution (ScyTek Laboratories, ACJ500) until the staining could be visualized. Excess AEC solution was then washed off with deionized water, and the slides were counterstained with hematoxylin (Fisher Scientific, 353032). Excess hematoxylin was removed by submersing the slides in deionized water. Stained tissue was then covered with Clear-Mount (Electron Microscopy Science, 17985-15) and heated at 54°C to protect the tissue from the organic solvents in the cover slip media. Cover slips were then attached with Permaslip mounting medium (Alban Scientific, A325A).

Tissue Analysis

Each eye was coded prior to sample analysis. This allowed the examiner to be masked to sample age and identity. While the examiner was masked to the age of the sample, it was impossible to fully mask the examiner because young eyes appeared smaller and old eyes appeared larger. Stained tissue sections were visualized with a live view with an Olympus BX51 microscope with the 4x objective. No still images were obtained for the purpose of determining ciliary muscle lengths and volumes because the analysis software was not capable of performing this operation. Nevertheless, image resolution can be assumed to be similar to that of images on the pen input display computer screen (4x = 520 pixels/mm). The area of each stained ciliary muscle section was traced using a pen input display computer screen (Wacom, Cintiq 21UX) and Stereo Investigator 9.0 software (MBF Bioscience) (Figure 2). The masked examiner used the pen to manually trace the ciliary muscle sections. The software only allowed for continuous tracings to be performed, which means that editing to correct minor errors during ciliary muscle tracings was not possible. The Stereo Investigator data were then analyzed with NeuroLucida Explorer (MBF Bioscience) to obtain the final cross-sectional area measurements of each section.

Three ciliary muscles at each time-point were reconstructed by obtaining cross-sectional area measurements that were approximately 300 μ m apart. Ciliary muscle area tracings were then aligned with the Stereo Investigator and NeuroLucida Explorer was used to create three-dimensional reconstructions of the muscle. Ciliary muscle volumes were then determined via two methods. The first full reconstruction method used all sections and was only performed on the three eyes at each time-point used in the above three-dimensional reconstructions of the muscle. Ciliary muscle volume was also determined by a second

abbreviated method. The primary goal of developing a second method was to have a means of determining ciliary muscle volume in a much more efficient and cost-effective manner.

In the first, full reconstruction method, the area of each ciliary muscle cross section was determined as above. The average area of all cross sections was calculated and then multiplied by limbal circumference. Limbal circumference was chosen as the third dimensional multiplier in order to anchor all volumes to a pre-processing biometric measurement. In the second method, the means and standard deviations of increasing numbers of ciliary muscle sections (e.g., mean area and standard deviation of 2, 4, 6, etc. sections) were plotted to determine the lowest number of sections needed to determine an accurate ciliary muscle volume, i.e., to obtain a stable estimate of average ciliary muscle cross sectional area (Figure 3). This was performed for all 15 eyes used in the original analysis. An example of one of these plots can be found in Figure 3. Plots were then visually inspected, and 10 sections were determined to be an optimal number for future analysis. The use of histological analysis, which causes tissue alterations, and data averaging prohibits this method from obtaining absolute ciliary muscle length and volume measurements; therefore, all values obtained from this analysis technique must be considered to be relative measurements and not absolute measurements.

Statistical Analysis

Means and standard deviations provided descriptive statistics of general data trends. A Wilcoxon signed-rank test was used to compare the two ciliary muscle volume determination methods, and linear regression was used to compare ciliary muscle volume to eye length, equatorial diameter, refractive error, eye shape, and age. Multivariate regression was used to assess how the ciliary muscle was related to biometric variables such as ocular size and shape, refractive error, and age. Paired t-tests and Bland-Altman analysis was also used to assess ocular shape and ciliary muscle measurement repeatability.³³ Significance was set at the 0.05 level. Statistical calculations were determined with Microsoft Excel and Stata 12.0 software.

RESULTS

Refractive Error, Ocular Size, and Eye Shape

The overall mean refractive error of the guinea pigs across all ages was $+1.43 \pm 2.98$ D with the animals starting out highly hyperopic and becoming clinically emmetropic by about 90-days of age (Table 1). One exception to this trend was with the 10-day old guinea pigs, which were much more myopic (-2.21 ± 2.93 D) than the other age groups (Table 1). The guinea pigs' ocular lengths, equatorial diameters, and limbal circumferences across all ages can be found in Table 1. These values are comparable to the results obtained by Howlett and McFadden.²³ Again, in general, these values also tended to increase with age with the exception of the 10-day old eyes. Finally, the guinea pigs' overall mean ocular shape ratio (axial length/equatorial diameter) was 0.96 ± 0.02 across all ages (Table 1). An ocular shape ratio that is less than one indicates that the guinea pig eyes are wider equatorially than the eye is long. Overall, the guinea pig eyes were only slightly wider than long.

Data were also collected to test eye shape and the repeatability of the photometric analysis method. Paired t-tests indicated that there were no significant differences between occasions for any of the repeated best-fit circles (eye length [$P = 0.54$], coronal vertical circle [$P = 0.13$], coronal horizontal circle [$P = 0.15$], limbal vertical circle [$P = 0.55$], and limbal horizontal circles [$P = 0.46$]). Also, there were no significant differences between the coronal horizontal and vertical circles ($P = 0.84$) and between the limbal vertical and horizontal circles ($P = 0.92$), which means that the coronal view and that the limbus of the eyes are essentially circular. Bland-Altman analysis was also used to determine the method's repeatability.³³

Ciliary Muscle Reconstruction and Ciliary Muscle Volume

The ciliary muscle was successfully reconstructed at all five ages tested (Figures 2, 4, & 5), and the ciliary muscle tracing method was found to be repeatable in that the 95% limits of agreement were several times lower than the change with age for all variables (Table 2). The two ciliary muscle volume determination methods also yielded similar results (Figure 3; Wilcoxon signed-rank test; $P = 0.86$), so the abbreviated ciliary muscle volume determination method was applied to all 30 eyes and used in all subsequent analyses. The mean ciliary muscle volumes of the 1, 10, 20, 30, and 90-day old eyes were 0.40 ± 0.16 mm³, 0.48 ± 0.13 mm³, 0.67 ± 0.15 mm³, 0.86 ± 0.35 mm³, and 1.09 ± 0.63 mm³, respectively (Figure 6), a roughly 2.5 fold increase during normal development. Upon morphological observation, the ciliary muscle appeared to span its natural attachment points (ora serrata & scleral spur) at 1 day of age (Figure 7).³⁴ Visual determination was done in a similar manner to that of the Bailey laboratory.³⁵ Therefore, it appears that the muscle has reached its general conformation by the time of birth. After birth, the muscle then continues to grow longer and thicker as the eye grows with age (Figure 8 & 9). This growth was tracked by analyzing the longest length of each section, a measure that is directly taken from data output produced by NeuroLucida Explorer (Figure 8). Analysis of these data illustrates that ciliary muscle length increased about 48% over time. Ciliary muscle thickness was also determined by calculation because NeuroLucida Explorer does not provide a direct measure. Ciliary muscle average thickness was determined by dividing the average area of ten ciliary muscle sections by the average length of these sections at each age. The mean ciliary muscle thickness increased by about 47% over the first 90 days of life (Figure 9). Finally, only a small part of the overall increase in ciliary muscle volume resulted from an increase in ciliary muscle ring circumference; limbal circumference, the anterior attachment point of the ciliary muscle, only increased by 21% over the duration of the study (Table 1).

Ciliary muscle volume was significantly correlated with log age ($r = 0.57$; $P = 0.001$) (Figure 6). If ciliary muscle volume were to be plotted linearly against age, it would appear to plateau at around 90-days of age (graph not shown). When relating ciliary muscle volume with ocular length ($r = 0.52$; $P = 0.003$), equatorial diameter ($r = 0.53$; $P = 0.003$), and limbal circumference ($r = 0.46$; $P = 0.01$), all were significantly correlated. In contrast, refractive error ($P = 0.73$) and ocular shape were not statistically related to ciliary muscle volume ($P = 0.60$). In general, eyes were relatively oblate in shape, which was expected because the majority of the eyes had a hyperopic refractive error. Age appeared to be the common factor behind each of these correlations; multivariate regression determined that the ocular

biometric variables were not significantly associated with ciliary muscle volume after adjustment for log age.

DISCUSSION

There is some evidence to suggest that the ciliary muscle is involved in the development of myopia,^{8, 14–16} yet there is a dearth of information with regards to the biochemical process leading to the increased ciliary muscle thickness seen in myopic subjects. Specifically, this study was able to develop a method for quantifying the amount of muscle present in a guinea pig's eye, to track its morphological postnatal development, and to describe how this information was related to other developmental and biometric characteristics.

The use of three-dimensional tissue reconstruction is of note because it has been rarely used to describe the development of large biological structures. Nevertheless, after reviewing the literature, it is clear that this innovative technique is becoming more widely used. For example, it has been used to describe the shape and structure of the bladder and neurons.^{32, 36} It has also been recently used to describe structural changes in meibomian glands (Parfitt GJ, et al. *IOVS* 2012: ARVO E-Abstract 2671) and in the optic nerve head.³⁷

Likewise, while much is known about the unique histology of the ciliary muscle, there is little information on how its size changes over time.^{31, 34, 38} With regards to histology, it is known that the ciliary muscle is made of smooth muscle, yet it possesses characteristic of both smooth and skeletal muscle. For example, it has α -smooth muscle actin and dense bodies, which are primarily seen in smooth muscle.^{34, 39, 40} At the same time, it has numerous mitochondria, rough endoplasmic reticulum, and dense bands with a regular alignment, which is primarily seen skeletal muscle.^{34, 39} Furthermore, humans are able to voluntarily activate their ciliary muscle to produce accommodation; this feature is also more typical of skeletal muscle.⁴¹

With regards to ciliary muscle size, there has been little written about the overall amount of ciliary muscle present in various species. In an early paper, Woolf commented on the general relative amount of ciliary muscle present in different species.³¹ For example, he said that mammals have well developed ciliary muscles, squirrels and guinea pigs have moderately developed muscle, and that the muscle is poorly developed in most other animals studied.³¹ To the best of our knowledge, the present study is the first to quantitatively describe the relative volume of ciliary muscle present in an animal during development. Overall, the present study found that the mean ciliary muscle volume of a 90-day-old guinea pig was $1.09 \pm 0.63 \text{ mm}^3$, which is about a 2.5 fold increase in volume compared to a 1-day-old animal (Figure 6). This volume increase primarily resulted from the ciliary muscle getting thicker and longer, 47% and 48% respectively, with a smaller amount coming from an increase in ciliary muscle/limbal ring diameter (21%; Figures 8 & 9).

Nevertheless, there have been groups that have commented on the thickness of the ciliary body or muscle at different locations within the human eye. One of the first of these studies was performed by Oliveira and coworkers with ultrasound biomicroscopy.¹⁵ This study determined that the mean ciliary body thickness for myopes 2 mm and 3 mm posterior to the

scleral spur was $490 \pm 115 \mu\text{m}$ and $315 \pm 79 \mu\text{m}$ and the mean ciliary body thickness for hyperopes 2 mm and 3 mm posterior to the scleral spur was $317 \pm 77 \mu\text{m}$ and $224 \pm 53 \mu\text{m}$.¹⁵ They were also the first to determine that the posterior segment of the ciliary body was thicker in adult myopic subjects compared to the posterior segment of the ciliary body of non-myopic subjects.¹⁵ These results were later confirmed by Bailey and coworkers in children with optical coherence tomography (OCT).¹⁴ Specifically, they found that the mean ciliary muscle thickness was $899.43 \pm 121.71 \mu\text{m}$, $601.49 \pm 101.55 \mu\text{m}$, $326.27 \pm 69.85 \mu\text{m}$ at 1, 2, and 3 mm posterior to the scleral spur.¹⁴ Bailey and coworkers have since corroborated their own findings in children and adults (Ernst LE, et al. *IOVS* 2008;49: E-Abstract 3580).⁴² They have also determined that the anterior apical portion of the ciliary muscle is thicker in hyperopic subjects compared to myopic subjects.⁴²

While the present study's primary objective was to develop a method for tracking ciliary muscle volume during development, it also secondarily sought to obtain data on how ciliary muscle volume was related to biometric values like refractive error. Although our data are preliminary due to the small range in refractive errors studied, the present study did not find a significant association with refractive error ($P = 0.73$) while the above human studies did.^{14, 15, 42} These conclusions were drawn from a dataset that included, in some cases, more than one data point per animal. However, sub-analysis indicated that eyes from different animals within the same age group ($R^2 = 0.36$) were actually more correlated than the right and left eyes from the same animal ($R^2 = 0.08$); therefore, the assumption that each eye represented an independent observation seems reasonable.

Another major difference is that the guinea pigs used in this experiment are much younger than the subjects analyzed in the human studies.^{14,15,42} The effects of age may outweigh the effects of refractive error. The 10-day old age group analyzed in the present study was abnormally myopic compared to age norms (Table 1).²³ Another group has reported on spontaneously myopic guinea pigs, and it is not uncommon to find these animals in colonies.⁴³ Thus, it is possible that these animals could have skewed our results; therefore, we repeated the above linear and multivariate regression analyses without the 10-day old age group (data not shown). The subsequent linear regression results were essentially the same, except for refractive error, which was now significant, with less hyperopic refractive errors associated with thicker ciliary muscles ($r = -0.44$; $P = 0.03$). Nevertheless, refractive error was still not significant in multivariate regression, indicating that age was the primary predictor of ciliary muscle volume. The myopia in the 10-day-old age group may have been refractive in origin as the axial lengths in all age groups compared well to those reported for normal pigmented guinea pigs.²³ This hypothesis is supported by the fact that there was no relationship between refractive error and eye length within the sample of 10-day-old animals (Spearman's correlation; $P = 0.21$) while there was within the full dataset (Spearman's correlation; $P = 0.01$). Future work will evaluate the effect of induced refractive error on guinea pig ciliary muscle volume in comparison to the normal development in the current study. This work along with studying a group of animals with a larger range of refractive errors is needed before the relationship between a guinea pig's ciliary muscle volume and refractive error can be fully determined.

The present study also analyzed age and secondary factors such as eye size and eye shape (Table 1). Specifically, the present study determined that ciliary muscle volume was significantly correlated with log age ($P = 0.001$), ocular length ($P = 0.003$), equatorial diameter ($P = 0.003$), and limbal circumference ($P = 0.01$). It also determined that the ciliary muscle was not associated with eye shape ($P = 0.60$). Finally, multivariate regression determined that the ocular biometric variables were not significantly associated with ciliary muscle volume after adjustment for age; therefore, each of these significant biometric measures were being driven, or merely developing, in tandem with age. Previous human studies have also found a similar association with age and eye size (axial length).^{14, 42, 44} To the best of our knowledge, no one has specifically reported on how eye shape is related to ciliary muscle thickness and/or volume. Since the current study analyzed enucleated eyes, it is possible that we did not find an association because we have altered the eyes from their normal state. This limitation may also apply to eye size; therefore, future work should be confirmed with less invasive means (e.g., magnetic resonance imaging or OCT). The lack of an association between ciliary muscle volume and factors other than age in multivariate regression is perhaps not surprising during normal development. This finding also leads to the next line of experimentation, which is the determination of how lens- or form deprivation-induced myopia (abnormal animals) alters the ciliary muscle and how these values are related to refractive error and ocular length.^{3, 4, 28, 45, 46}

While this study does have a number of strengths, it is not without its limitations. The primary limitation to this study is that the methods used to determine ciliary muscle volume are only able to provide relative measurements. This is because tissue sectioning, processing, and staining are known to cause tissue shrinkage and/or distortions.^{36, 47} Some of these distortions can be seen visually in our data (Figure 2 & 7). The observed distortions may appear significant, yet they appear consistently among the eyes across ages; as a result, we believed that this limitation is not preventing us from determining useful relative volume measurements. This pitfall is unavoidable in histology, and it is widely accepted by the community.^{36, 47} In order to compensate for this limitation, researchers have used correction factors to partially negate this problem.³⁶ The present study has also attempted to employ a correction factor; this was done by anchoring each ciliary muscle volume to each eye's limbal circumference. Admittedly, anchoring volume measurements to the limbus is also a limitation because it too is only an estimate of the true origin of the ciliary muscle. Again, less invasive imaging methods will be useful for evaluating these potential histological artifacts.

In conclusion, the above data demonstrate that ciliary muscle volume, length, and thickness increase robustly with age during the 90 days required to reach adult refractive error and axial length. The ciliary muscle appears to undergo active development after birth as opposed to passively occupying the space between its attachments. Initial data demonstrate that ciliary muscle volume is primarily related to age in normal albino guinea pigs, yet additional studies are needed to confirm this conclusion. When considering these data as a whole, they provide evidence in favor of using the guinea pig to study the ciliary muscle in an animal myopia model because a normal ciliary muscle is not significantly related to normal biometric values in guinea pigs. Future studies are also needed to determine what processes are leading to the observed increase in muscle volume over time during normal

growth (e.g., hypertrophy, hyperplasia). A future goal would also be to determine if there are differences between pigmented and albino strains because it is possible that they could have slightly different ciliary muscle development patterns – even though Ostrin and coworkers reported that the two strains have similar visual acuities and Vingrys and Bui reported that they have similar electroretinogram patterns (Ostrin LA, et al. *IOVS* 2011: ARVO E-Abstract 6296).⁴⁸ Finally, studies are needed to determine if lens-or form-deprivation experiments are able to cause exaggerated ciliary muscle growth through the same or through a different mechanism compared to that driving growth during normal development.

Acknowledgments

Research reported in this publication was supported by the National Eye Institute of the National Institutes of Health under Award Number EY08893 (CLEERE Study). The content is solely the responsibility of the authors and does not necessarily represent the official views of the National Institutes of Health. This research was also supported by the E. F. Wildermuth Foundation fund.

The authors would like to thank the American Optometric Foundation's William C. Ezell Fellowship program for financial support during the development of this project. The authors would also like to thank the Andrew Fischer, PhD laboratory for their generous laboratory support during the implementation of this project and Mackenzie Nicolaus, BS for helping with the management of the animal colony.

References

1. Lu F, Zhou X, Jiang L, Fu Y, Lai X, Xie R, Qu J. Axial myopia induced by hyperopic defocus in guinea pigs: A detailed assessment on susceptibility and recovery. *Exp Eye Res.* 2009; 89:101–8. [PubMed: 19268468]
2. Troilo D, Quinn N, Baker K. Accommodation and induced myopia in marmosets. *Vision Res.* 2007; 47:1228–44. [PubMed: 17360018]
3. Smith EL 3rd, Hung LF. The role of optical defocus in regulating refractive development in infant monkeys. *Vision Res.* 1999; 39:1415–35. [PubMed: 10343811]
4. Howlett MH, McFadden SA. Spectacle lens compensation in the pigmented guinea pig. *Vision Res.* 2009; 49:219–27. [PubMed: 18992765]
5. Lawrence MS, Azar DT. Myopia and models and mechanisms of refractive error control. *Ophthalmol Clin North Am.* 2002; 15:127–33. [PubMed: 12064076]
6. Pediatric Eye Disease Investigator Group. Progressive-addition lenses versus single-vision lenses for slowing progression of myopia in children with high accommodative lag and near esophoria. Correction of Myopia Evaluation Trial 2. *Invest Ophthalmol Vis Sci.* 2011; 52:2749–57. [PubMed: 21282579]
7. Gwiazda J, Hyman L, Hussein M, Everett D, Norton TT, Kurtz D, Leske MC, Manny R, Marsh-Tootle W, Scheiman M. A randomized clinical trial of progressive addition lenses versus single vision lenses on the progression of myopia in children. *Invest Ophthalmol Vis Sci.* 2003; 44:1492–500. [PubMed: 12657584]
8. Mutti DO, Mitchell GL, Hayes JR, Jones LA, Moeschberger ML, Cotter SA, Kleinstein RN, Manny RE, Twelker JD, Zadnik K. Accommodative lag before and after the onset of myopia. *Invest Ophthalmol Vis Sci.* 2006; 47:837–46. [PubMed: 16505015]
9. Smith EL 3rd. Prentice Award Lecture 2010: A case for peripheral optical treatment strategies for myopia. *Optom Vis Sci.* 2011; 88:1029–44. [PubMed: 21747306]
10. Mutti DO, Hayes JR, Mitchell GL, Jones LA, Moeschberger ML, Cotter SA, Kleinstein RN, Manny RE, Twelker JD, Zadnik K. Refractive error, axial length, and relative peripheral refractive error before and after the onset of myopia. *Invest Ophthalmol Vis Sci.* 2007; 48:2510–9. [PubMed: 17525178]
11. Walline JJ, Jones LA, Sinnott LT. Corneal reshaping and myopia progression. *Br J Ophthalmol.* 2009; 93:1181–5. [PubMed: 19416935]

12. Cho P, Cheung SW, Edwards M. The longitudinal orthokeratology research in children (LORIC) in Hong Kong: a pilot study on refractive changes and myopic control. *Curr Eye Res.* 2005; 30:71–80. [PubMed: 15875367]
13. Atchison DA, Pritchard N, Schmid KL, Scott DH, Jones CE, Pope JM. Shape of the retinal surface in emmetropia and myopia. *Invest Ophthalmol Vis Sci.* 2005; 46:2698–707. [PubMed: 16043841]
14. Bailey MD, Sinnott LT, Mutti DO. Ciliary body thickness and refractive error in children. *Invest Ophthalmol Vis Sci.* 2008; 49:4353–60. [PubMed: 18566470]
15. Oliveira C, Tello C, Liebmann JM, Ritch R. Ciliary body thickness increases with increasing axial myopia. *Am J Ophthalmol.* 2005; 140:324–5. [PubMed: 16086961]
16. Gwiazda J, Thorn F, Held R. Accommodation, accommodative convergence, and response AC/A ratios before and at the onset of myopia in children. *Optom Vis Sci.* 2005; 82:273–8. [PubMed: 15829855]
17. Mutti DO, Jones LA, Moeschberger ML, Zadnik K. AC/A ratio, age, and refractive error in children. *Invest Ophthalmol Vis Sci.* 2000; 41:2469–78. [PubMed: 10937556]
18. Mutti DO, Mitchell GL, Sinnott LT, Jones-Jordan LA, Moeschberger ML, Cotter SA, Kleinstein RN, Manny RE, Twelker JD, Zadnik K, Group CS. Corneal and crystalline lens dimensions before and after myopia onset. *Optom Vis Sci.* 2012; 89:251–62. [PubMed: 22227914]
19. Mutti DO, Zadnik K, Fusaro RE, Friedman NE, Sholtz RI, Adams AJ. Optical and structural development of the crystalline lens in childhood. *Invest Ophthalmol Vis Sci.* 1998; 39:120–33. [PubMed: 9430553]
20. Zadnik K, Mutti DO. How applicable are animal myopia models to human juvenile onset myopia? *Vision Res.* 1995; 35:1283–8. [PubMed: 7610588]
21. May CA, Skorski LM, Lutjen-Drecoll E. Innervation of the porcine ciliary muscle and outflow region. *J Anat.* 2005; 206:231–6. [PubMed: 15733294]
22. Ebersberger A, Flugel C, Lutjen-Drecoll E. Ultrastructural and enzyme histochemical studies of regional structural differences within the ciliary muscle in various species. *Klin Monbl Augenheilkd.* 1993; 203:53–8. [PubMed: 8411892]
23. Howlett MH, McFadden SA. Emmetropization and schematic eye models in developing pigmented guinea pigs. *Vision Res.* 2007; 47:1178–90. [PubMed: 17360016]
24. Ates K, Demirtas S, Goksoy C. Binocular interactions in the guinea pig's visual-evoked potentials. *Brain Res.* 2006; 1125:26–30. [PubMed: 17112481]
25. Zhou JB, Ge S, Gu P, Peng D, Chen GF, Pan MZ, Qu J. Microdissection of guinea pig extraocular muscles. *Exp Ther Med.* 2011; 2:1183–5. [PubMed: 22977641]
26. Tedesco RC, Calabrese KS, Smith RL. Architecture of the ciliary muscle of *Gallus domesticus*. *Anat Rec (A) Discov Mol Cell Evol Biol.* 2005; 284:544–9. [PubMed: 15830343]
27. Glasser A, Murphy CJ, Troilo D, Howland HC. The mechanism of lenticular accommodation in chicks. *Vision Res.* 1995; 35:1525–40. [PubMed: 7667911]
28. Howlett MH, McFadden SA. Form-deprivation myopia in the guinea pig (*Cavia porcellus*). *Vision Res.* 2006; 46:267–83. [PubMed: 16139323]
29. He JC, Burns SA, Marcos S. Monochromatic aberrations in the accommodated human eye. *Vision Res.* 2000; 40:41–8. [PubMed: 10768040]
30. Vilupuru AS, Roorda A, Glasser A. Spatially variant changes in lens power during ocular accommodation in a rhesus monkey eye. *J Vis.* 2004; 4:299–309. [PubMed: 15134477]
31. Woolf D. A comparative cytological study of the ciliary muscle. *Anat Rec.* 1956; 124:145–63. [PubMed: 13302815]
32. Carpenter A, Paulus A, Robinson M, Bates CM, Robinson ML, Hains D, Kline D, McHugh KM. 3-Dimensional morphometric analysis of murine bladder development and dysmorphogenesis. *Dev Dyn.* 2012; 241:522–33. [PubMed: 22275180]
33. Bland JM, Altman DG. Statistical methods for assessing agreement between two methods of clinical measurement. *Lancet.* 1986; 1:307–10. [PubMed: 2868172]
34. Tamm ER, Lutjen-Drecoll E. Ciliary body. *Microsc Res Tech.* 1996; 33:390–439. [PubMed: 8695897]

35. Kao CY, Richdale K, Sinnott LT, Grillott LE, Bailey MD. Semiautomatic extraction algorithm for images of the ciliary muscle. *Optom Vis Sci.* 2011; 88:275–89. [PubMed: 21169877]
36. Marx M, Gunter RH, Hucko W, Radnikow G, Feldmeyer D. Improved biocytin labeling and neuronal 3D reconstruction. *Nat Protoc.* 2012; 7:394–407. [PubMed: 22301777]
37. Burgoyne CF, Downs JC, Bellezza AJ, Hart RT. Three-dimensional reconstruction of normal and early glaucoma monkey optic nerve head connective tissues. *Invest Ophthalmol Vis Sci.* 2004; 45:4388–99. [PubMed: 15557447]
38. Kaufman, PL.; Alm, A.; Adler, FH., editors. *Adler's Physiology of the Eye: Clinical Application.* 10. St. Louis: Mosby; 2003.
39. Tortora, GJ.; Grabowski, SR. *Principles of Anatomy and Physiology.* 10. New York: Wiley; 2003.
40. Roby T, Olsen S, Nagatomi J. Effect of sustained tension on bladder smooth muscle cells in three-dimensional culture. *Ann Biomed Eng.* 2008; 36:1744–51. [PubMed: 18683053]
41. Lossing LA, Sinnott LT, Kao CY, Richdale K, Bailey MD. Measuring changes in ciliary muscle thickness with accommodation in young adults. *Optom Vis Sci.* 2012; 89:719–26. [PubMed: 22504328]
42. Pucker AD, Sinnott LT, Kao CY, Bailey MD. Region-specific relationships between refractive error and ciliary muscle thickness in children. *Invest Ophthalmol Vis Sci.* 2013; 54:4710–6. [PubMed: 23761093]
43. Ren Y, Xie R, Zhou X, Pan M, Lu F. Spontaneous high myopia in one eye will affect the development of form deprivation myopia in the fellow eye. *Curr Eye Res.* 2011; 36:513–21. [PubMed: 21591860]
44. Muftuoglu O, Hosal BM, Zilelioglu G. Ciliary body thickness in unilateral high axial myopia. *Eye (Lond).* 2009; 23:1176–81. [PubMed: 18551140]
45. Smith EL 3rd, Hung LF, Huang J. Relative peripheral hyperopic defocus alters central refractive development in infant monkeys. *Vision Res.* 2009; 49:2386–92. [PubMed: 19632261]
46. Wiesel TN, Raviola E. Myopia and eye enlargement after neonatal lid fusion in monkeys. *Nature.* 1977; 266:66–8. [PubMed: 402582]
47. Hatton WJ, von Bartheld CS. Analysis of cell death in the trochlear nucleus of the chick embryo: calibration of the optical disector counting method reveals systematic bias. *J Comp Neurol.* 1999; 409:169–86. [PubMed: 10379913]
48. Vingrys AJ, Bui BV. Development of postreceptoral function in pigmented and albino guinea pigs. *Vis Neurosci.* 2001; 18:605–13. [PubMed: 11829306]

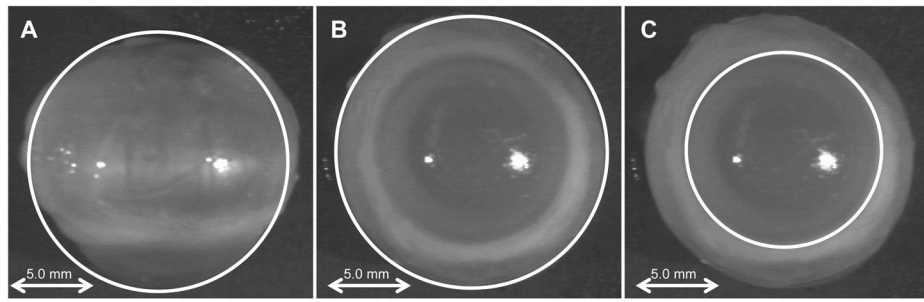


Figure 1. Examples of best-fit circles for determining structural areas. Note that white lines are outlining examples of the coronal (A), transverse (B), and limbal (C) areas.

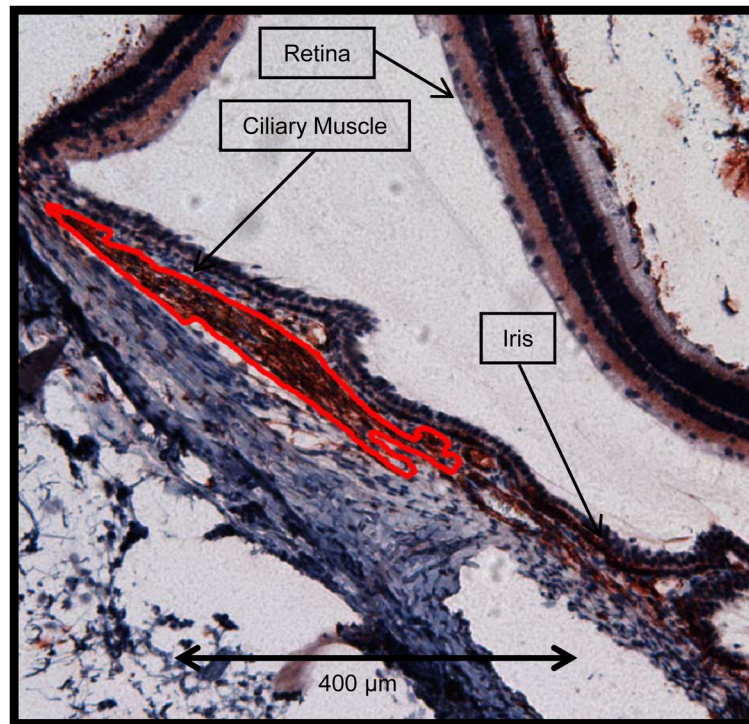


Figure 2.
An example tracing of stained ciliary muscle. Note that the ciliary muscle is outlined in red (10x objective).

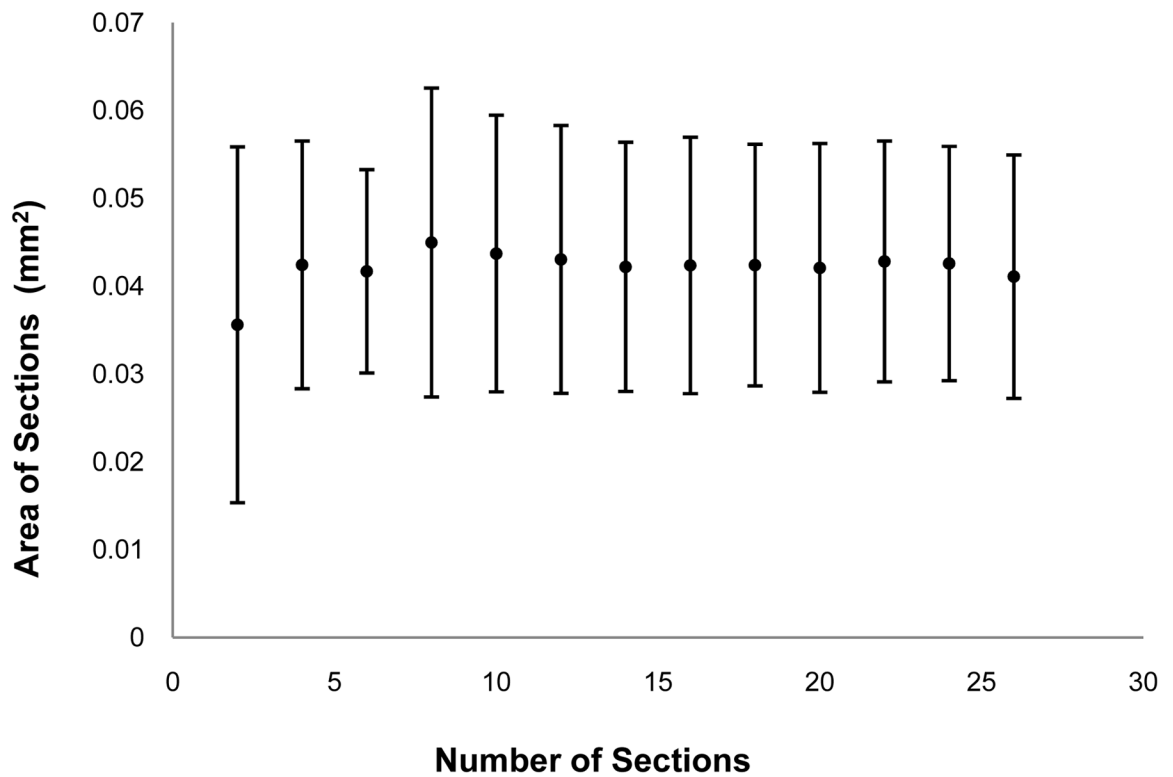


Figure 3. Determination of optimal number of ciliary muscle sections. The mean area of ciliary muscle sections are plotted with an increasing number of sections at each point. Note that the mean area is approximately stable with ten or more sections and that each side of an error bar represents one standard deviation from the mean.

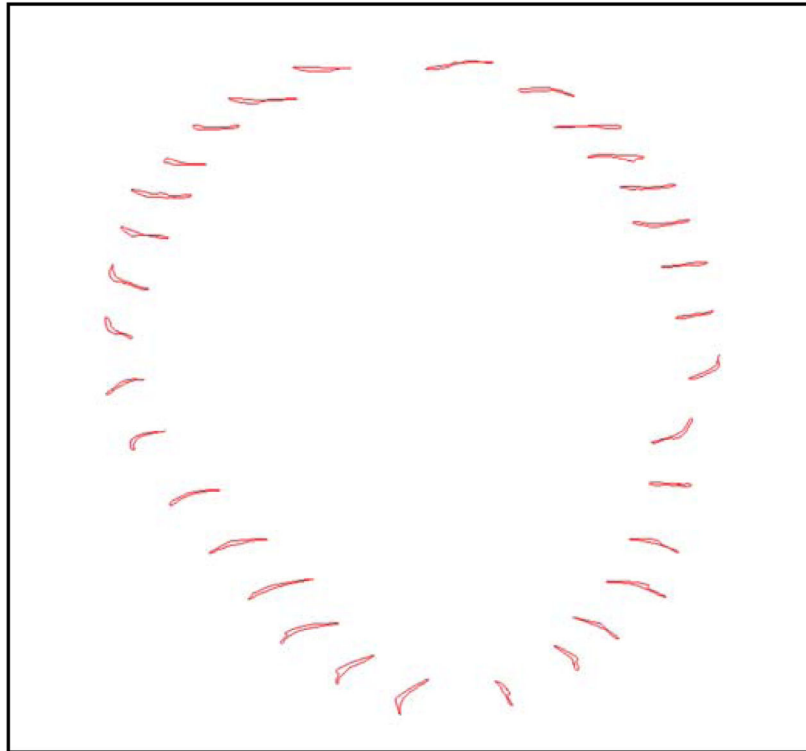


Figure 4. An example of stacked ciliary muscle sections prior to computer generated three-dimensional reconstruction. Note how tracings like seen in Figure 2 are taken from throughout the entire eye, stacked, and aligned to allow for three-dimensional reconstruction of the ciliary muscle.

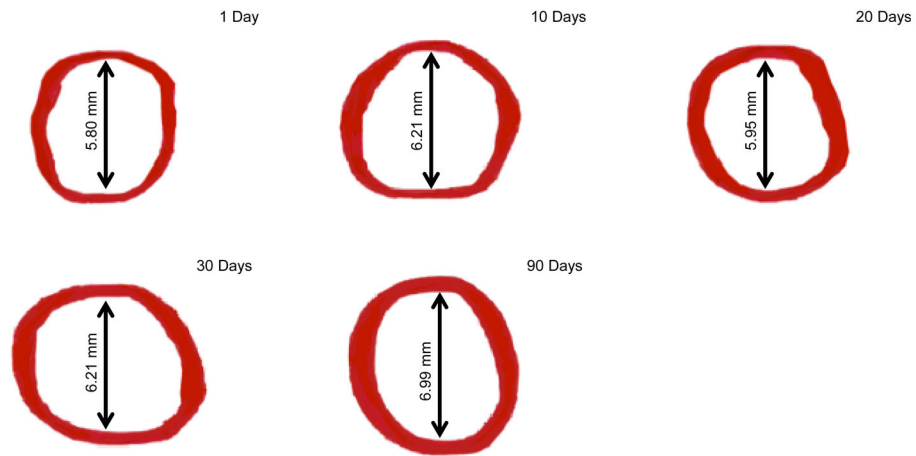


Figure 5. Reconstructed images of ciliary muscle volume at 1, 10, 20, 30, and 90 days of age. Note that each arrow and associated value represents the mean inner ciliary muscle ring diameter at the listed time-point. Also note that superior and inferior ring thinning can be seen in some images; this artifact is due to the software during the reconstruction process.

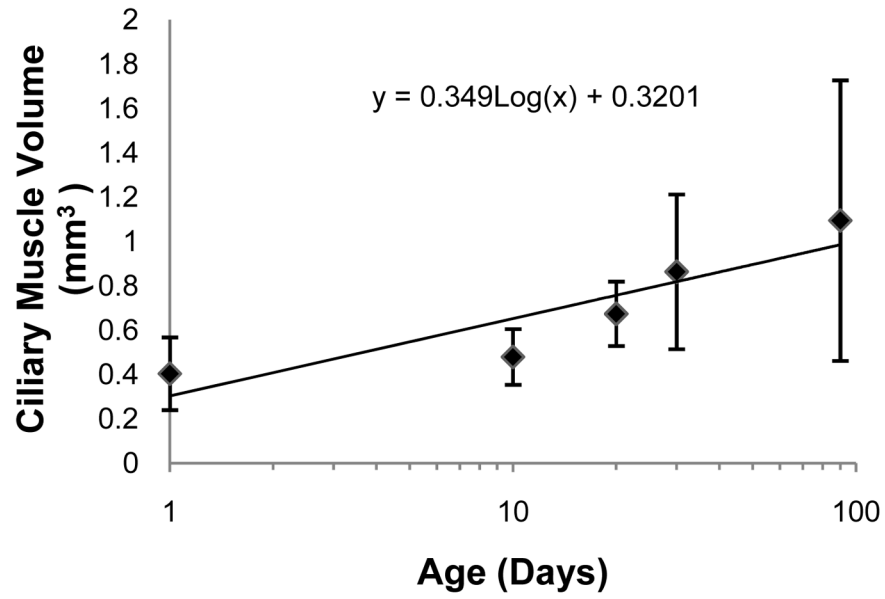


Figure 6. Ciliary muscle volume at different ages. The presented data are best represented as a log growth pattern ($R^2 = 0.81$). Each side of an error bar represents one standard deviation from the mean.

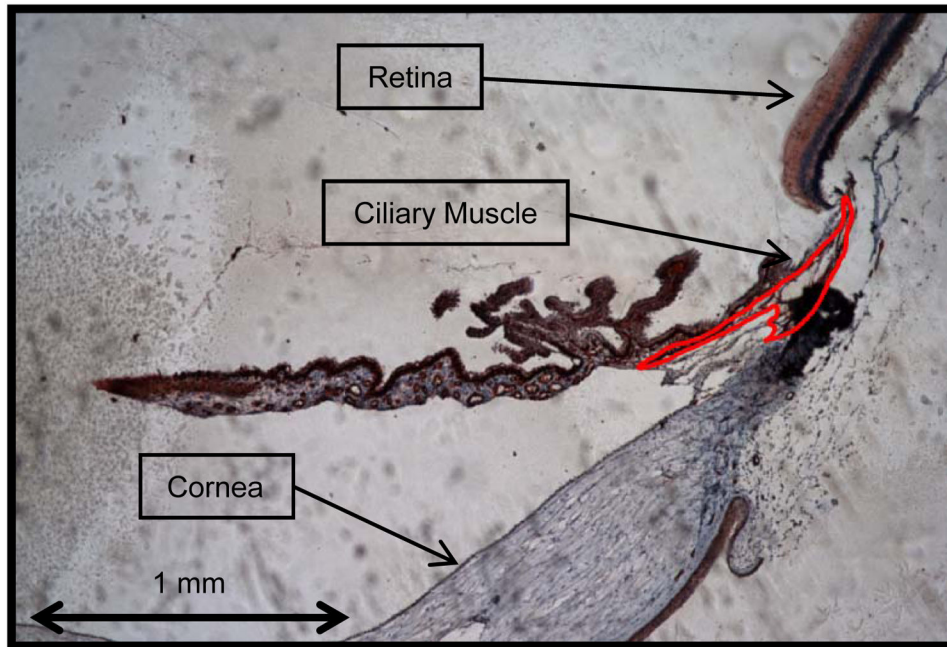


Figure 7.
An example picture of 1-day-old guinea pig ciliary muscles. Note that the ciliary muscle spans its natural attachment points at 1 day of age (4x objective).

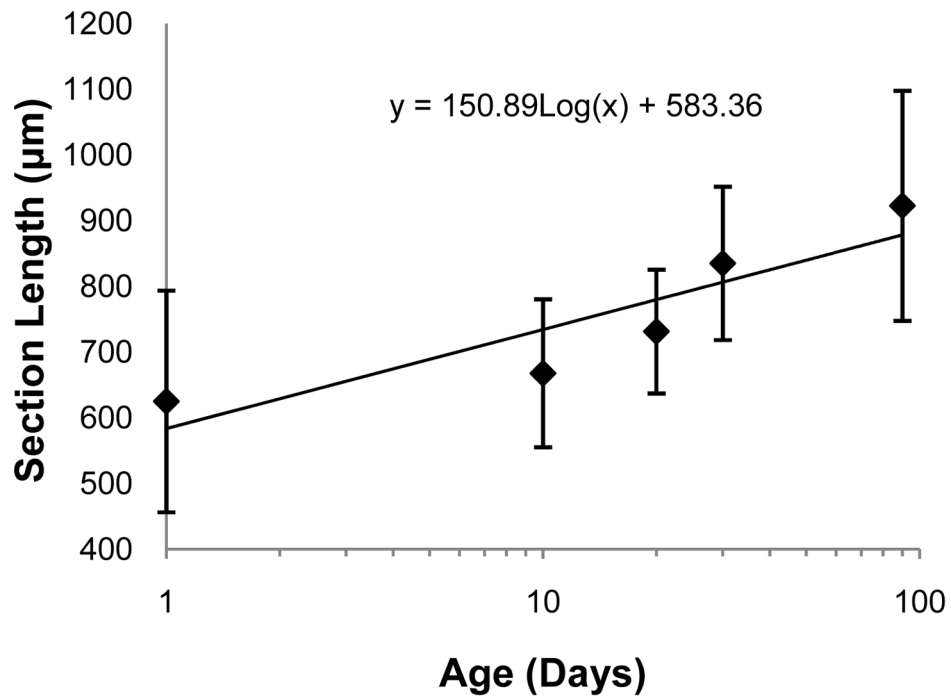


Figure 8. Length of ciliary muscle sections over time. The presented data are best represented as a log growth pattern ($R^2 = 0.81$). Each side of an error bar represents one standard deviation from the mean.

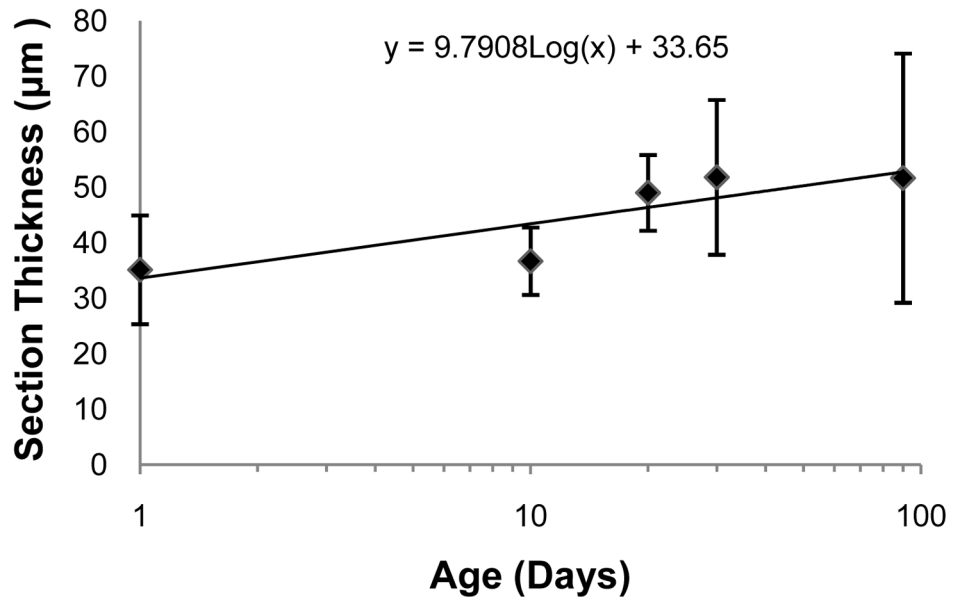


Figure 9. An Estimate of Mean Ciliary Muscle Thickness Over Time. The presented data are best represented as a log growth pattern ($R^2 = 0.75$). Each side of an error bar represents one standard deviation from the mean.

Table 1

Summary of Refractive Error, Ocular Shape, and Ciliary Muscle Volume ($n = 6$ eyes per age group).

	1 Day	10 Days	20 Days	30 Days	90 Days
Refractive Error (D)	+5.79 ± 1.47	-2.21 ± 2.93	+1.25 ± 0.76	+1.55 ± 0.87	+0.78 ± 0.73
Ocular Length (mm)	7.86 ± 0.20	8.48 ± 0.16	8.36 ± 0.16	8.86 ± 0.13	9.44 ± 0.27
Equatorial Diameter (mm)	8.33 ± 0.07	8.80 ± 0.13	8.56 ± 0.10	9.13 ± 0.14	9.86 ± 0.11
Limbal Circumference (mm)	18.21 ± 0.59	19.5 ± 0.26	18.67 ± 0.52	19.49 ± 0.31	21.96 ± 0.39
Ocular Shape (eye length/equatorial diameter)	0.94 ± 0.02	0.96 ± 0.01	0.98 ± 0.01	0.97 ± 0.01	0.96 ± 0.02
Ciliary Muscle Section Area (mm ²)	0.02 ± 0.01	0.02 ± 0.01	0.04 ± 0.01	0.04 ± 0.01	0.05 ± 0.03
Ciliary Muscle Volume (mm ³)	0.40 ± 0.16	0.48 ± 0.13	0.67 ± 0.15	0.86 ± 0.35	1.09 ± 0.63

Table 2

Summary of Bland-Altman Repeatability of Methods Analysis.

Measurement	Reliability (95% Limits of Agreement)
Ocular Length	± 0.25 (mm)
Equatorial Diameter	± 0.14 (mm)
Limbal Circumference	± 0.38 (mm)
Ciliary Muscle Section Area	± 0.012 (mm ²)
Ciliary Muscle Volume	± 0.26 (mm ³)